

Published in final edited form as:

Bioorg Med Chem Lett. 2013 March 15; 23(6): 1612–1616. doi:10.1016/j.bmcl.2013.01.106.

Synthesis and bioevaluation of [¹⁸F]4-fluoro-*m*-hydroxyphenethylguanidine ([¹⁸F]4F-MHPG): a novel radiotracer for quantitative PET studies of cardiac sympathetic innervation

Keun Sam Jang, Yong-Woon Jung, Phillip S. Sherman, Carole A. Quesada, Guie Gu, and David M. Raffel*

Division of Nuclear Medicine, Department of Radiology, 2276 Medical Science I Building, University of Michigan Medical School, Ann Arbor, Michigan 48109

Abstract

A new cardiac sympathetic nerve imaging agent, [¹⁸F]4-fluoro-*m*-hydroxyphenethylguanidine ([¹⁸F]4F-MHPG), was synthesized and evaluated. The radiosynthetic intermediate [¹⁸F]4-fluoro-*m*-tyramine ([¹⁸F]4F-MTA) was prepared and then sequentially reacted with cyanogen bromide and NH₄Br/NH₄OH to afford [¹⁸F]4F-MHPG. Initial bioevaluations of [¹⁸F]4F-MHPG (biodistribution studies in rats and kinetic studies in the isolated rat heart) were similar to results previously reported for the carbon-11 labeled analog [¹¹C]4F-MHPG. The neuronal uptake rate of [¹⁸F]4F-MHPG into the isolated rat heart was 0.68 ml/min/g wet and its retention time in sympathetic neurons was very long ($T_{1/2} > 13$ h). A PET imaging study in a nonhuman primate with [¹⁸F]4F-MHPG provided high quality images of the heart, with heart-to-blood ratios at 80–90 min after injection of 5-to-1. These initial kinetic and imaging studies of [¹⁸F]4F-MHPG suggest that this radiotracer may allow for more accurate quantification of regional cardiac sympathetic nerve density than is currently possible with existing neuronal imaging agents.

Keywords

Sympathetic nervous system; Metaiodobenzylguanidine; Hydroxyephedrine; Norepinephrine transporter

Radiiodinated *m*-iodobenzylguanidine (MIBG, Figure 1) was one of the first radiopharmaceuticals developed for scintigraphic imaging of presynaptic sympathetic nerve fibers in the human heart.¹ Clinical studies with MIBG have demonstrated significant changes in the regional distribution of cardiac sympathetic nerves in many diseases, including congestive heart failure, diabetic autonomic neuropathy, myocardial infarction, cardiac arrhythmias, sudden cardiac death and Parkinson's disease.² Several radiotracers for noninvasive imaging of cardiac sympathetic innervation with positron emission tomography (PET) have also been developed, including [¹¹C]-(-)-*m*-hydroxyephedrine ([¹¹C]HED, Figure 1),³ [¹¹C]-(-)-epinephrine ([¹¹C]EPI, Figure 1),⁴ [¹¹C]-(-)-

© 2013 Elsevier Ltd. All rights reserved.

*To whom correspondence should be address: David M. Raffel, Ph. D., Division of Nuclear Medicine, Department of Radiology, 2276 Medical Science I Building, 1301 Catherine Street, University of Michigan Medical School, Ann Arbor, Michigan 48109, Tel: (734) 936-0725, Fax: (734) 764-0288, raffel@umich.edu.

Publisher's Disclaimer: This is a PDF file of an unedited manuscript that has been accepted for publication. As a service to our customers we are providing this early version of the manuscript. The manuscript will undergo copyediting, typesetting, and review of the resulting proof before it is published in its final citable form. Please note that during the production process errors may be discovered which could affect the content, and all legal disclaimers that apply to the journal pertain.

phenylephrine,⁵ 6-¹⁸F]fluorometaraminol ([¹⁸F]6-FMR Figure 1),⁶ 6-¹⁸F]fluorodopamine,⁷ *m*-⁷⁶Br]bromobenzylguanidine⁸ and *p*-¹⁸F]fluorobenzylguanidine ([¹⁸F]PFBG).⁹

All of these tracers are structural analogs of the neurotransmitter norepinephrine. They are initially transported into cardiac sympathetic neurons as substrates of the norepinephrine transporter (NET). Once inside the neurons, to varying degrees these compounds are taken up into norepinephrine storage vesicles by the second isoform of the vesicular monoamine transporter (VMAT2).¹⁰ While the rapid neuronal uptake of these agents results in high quality images of the heart, this also causes problems in extracting accurate quantitative measures of regional sympathetic nerve density from the myocardial kinetics of these agents. NET transport of these tracers is a fast process and because of this their neuronal uptake rates are rate-limited by delivery from plasma to the extracellular spaces near the neurons. Extraction of these tracers from plasma is governed primarily by blood flow, so radiotracers with these kinetic properties are often called 'flow-limited tracers'. Since NET transport is not the rate-limiting step in the uptake of the tracer, it is not possible to extract an estimate of NET transport rate of the tracer from its myocardial kinetics, as measured from the acquired PET scan data. This is unfortunate, since a regional estimate of the NET transport rate of the tracer would likely serve as a sensitive measure of the regional density of presynaptic nerve terminals. The inability to apply tracer kinetic analysis approaches forces us to rely instead on semi-quantitative measures of tracer retention, such as the heart-to-mediastinum ratio (HMR) for MIBG and the retention index (RI) for [¹¹C]HED.¹⁰ While these have been found to be useful, another consequence of the rapid neuronal uptake rate of these compounds is that measures of tracer retention tend to be insensitive to regional nerve losses until those losses become fairly severe. Thus current tracers likely do not detect early denervation – which may be important in providing therapies designed to halt further cardiac denervation.

The only way to overcome these obstacles to accurate and sensitive detection of cardiac denervation is to develop a new tracer that possesses optimal kinetics for tracer kinetic analyses. Such tracers would provide more accurate and sensitive measures of regional nerve density, allowing detection of denervation earlier in the course of diseases that cause nerve damage, such as diabetic autonomic neuropathy and heart failure. We hypothesized that a new radiolabeled NET substrate should possess two kinetic properties to be better suited for tracer kinetic analyses: (1) a slower neuronal uptake rate; and (2) a very long neuronal retention time, through efficient vesicular storage. We believed that compounds with these kinetic properties could be found among the various guanidine derivatives that show potent pharmacological effects on cardiac sympathetic neurons. In particular, we chose to study phenethylguanidines because some of these compounds are known to be potent depletors of cardiac norepinephrine stores *in vivo*, due to their avid uptake and retention inside norepinephrine storage vesicles.¹¹

Evaluations of a series of carbon-11 labeled phenethylguanidines have previously been reported.¹² Among the compounds tested, [¹¹C]-4-fluoro-*m*-hydroxy-phenethylguanidine ([¹¹C]4F-MHPG, Figure 1) was found to possess the desired kinetic properties of a slower NET transport rate and a very long neuronal retention time. Also, microPET studies in rhesus macaque monkeys demonstrated that this agent had favorable *in vivo* imaging properties and kinetics. These encouraging results led us to attempt the synthesis of fluorine-18 labeled 4-fluoro-*m*-hydroxy-phenethylguanidine ([¹⁸F]4F-MHPG). While the short half-life of carbon-11 (20.1 min) limits its wide spread application due to the requirement of an on-site cyclotron, the longer half-life of fluorine-18 (109.8 min) allows for imaging studies at imaging centers without a cyclotron through distribution by commercial vendors. The longer half-life of fluorine-18 also allows for imaging times up to several

hours after injection into a patient and permits multiple patients doses to be dispensed from a single synthesis batch.

We describe here the preparation of a new fluorine-18 radiotracer ($[^{18}\text{F}]4\text{F-MHPG}$) for imaging cardiac sympathetic innervation with PET and the results of initial bioevaluation studies in rats and a non-human primate. Biological data for $[^{18}\text{F}]4\text{F-MHPG}$ are compared to previous results obtained with $[^{11}\text{C}]4\text{F-MHPG}$.

Reference standards for HPLC and *in vitro* studies, 4F-MHPG **1** and 4-fluoro-*m*-tyramine (4F-MTA, **7**), were prepared from the starting material 3-benzyloxy-4-fluorobenzaldehyde **2** (Scheme 1). The benzaldehyde **2** was reduced with NaBH_4 to afford the benzyl alcohol **3**. The alcohol **3** was converted to the benzyl bromide **4** by reaction with PBr_3 and then followed by treatment with sodium cyanide in DMSO to generate the benzyl cyanide **5**. Reduction of cyano group with borane and deprotection of the benzyl group with 48% HBr was carried out to provide 4F-MTA **7**. Condensation of 4F-MTA with 1,3-bis(*tert*-butoxycarbonyl)-2-methyl-2-thiopseudourea¹³ and then followed by deprotection under mild acidic condition afforded 4FMHPG **1**. Another reference standard, 3-benzyloxy-4-fluoro- β -nitrostyrene **12**, was prepared by the condensation of 3-benzyloxy-4-fluorobenzaldehyde **2** with nitromethane in the presence of ammonium acetate and glacial acetic acid (Scheme 2).¹⁴ The precursor for labeling of $[^{18}\text{F}]4\text{FMHPG}$, 3-benzyloxy-4-formyl-*N,N,N*-trimethylanilinium trifluoromethanesulfonate **10**, was synthesized according to the previously published method.¹⁵ 3-Benzyloxy-4-fluorobenzaldehyde **2** was converted to the dimethylamine **9** in 82% yield by the nucleophilic substitution reaction of fluorine with Me_2NH . The quarternary salt **10** was obtained in 71% yield by the treatment of **9** with methyl trifluoromethanesulfonate at room temperature under nitrogen.

Synthesis of the target compound $[^{18}\text{F}]4\text{F-MHPG}$ is shown in Scheme 2. This approach is based on previously established methods adapted from syntheses of $[^{11}\text{C}]$ tyramine¹⁶ and 6- $[^{18}\text{F}]$ fluorodopamine.¹⁷ The synthesis of $[^{18}\text{F}]4\text{F-MHPG}$ was started by production of $[^{18}\text{F}]$ benzaldehyde **11** through a no-carrier-added nucleophilic aromatic substitution reaction with $\text{K}[^{18}\text{F}]\text{F-K}_{2,2,2}$ with the precursor 3-benzyloxy-4-formyl-*N,N,N*-trimethylanilinium triflate **10**. The trimethylanilinium group in benzaldehyde afforded high incorporation of $[^{18}\text{F}]$ fluoride in the nucleophilic aromatic substitution reaction, providing a good radiochemical yield.¹⁵ In the second step, 4- $[^{18}\text{F}]$ fluoro-3-benzyloxybenzaldehyde **11** was condensed *in situ* with nitromethane in the presence of ammonium acetate/acetic acid/methanol to provide $[^{18}\text{F}]$ nitrostyrene **12**. The above two-step reaction was performed in a GE TRACERlab FX-N radiosynthesis module (GE HealthCare, Waukesha, WI, USA), with $15 \pm 4\%$ radiochemical yield and $>98\%$ radiochemical purity. The next step simultaneously reduced both the alkene group and nitro group of $[^{18}\text{F}]$ nitrostyrene. When lithium aluminum hydride (LAH) was used for this step, the reduction of both groups in **12** was not efficient. However, the sequential addition of borane followed by LAH increased the radiochemical yield. Cleavage of the benzyl ether protecting group with 48% HBr followed by HPLC purification afforded the intermediate 4- $[^{18}\text{F}]$ -fluoro-*m*-tyramine ($[^{18}\text{F}]4\text{F-MTA}$; **7**). The structure of the purified product was verified by comparing its retention time against a non-radioactive standard of 4F-MTA that was co-injected onto a reverse-phase HPLC column (Synergy Hydro 4 μ , 250 \times 4.6 mm, 5% EtOH in 60 mM NaH_2PO_4 , 1.2 ml/min, $R_t = 10.8$ min). In the final step, conversion of the primary amine of $[^{18}\text{F}]4\text{F-MTA}$ to a guanidine to form $[^{18}\text{F}]4\text{F-MHPG}$ was initially attempted by reacting the purified $[^{18}\text{F}]4\text{F-MTA}$ with 2-methyl-2-thiopseudourea sulfate, as previously reported.⁹ However, this reaction led to the formation of several radioactive impurities with low radiochemical yield. Use of other reagents such as cyanamide¹⁸ *N,N'*-bis(*t*-butoxycarbonyl)thiourea^{19, 20} and 1-guanyl-3,5-dimethylpyrazole²¹ were not successful. Although one of the most efficient methods reported in the literature seems to be treatment of *N,N'*-bis(*t*-butoxycarbonyl)thiourea with

mercuric chloride²², this reaction is not practical for a radiotracer that will be injected into non-human primates or humans due to the toxicity of mercuric sulfide produced as a side product. These initial findings led us to attempt a two-step reaction, first with cyanogen bromide, followed by treatment with $\text{NH}_4\text{Br}/\text{NH}_4\text{OH}$. This approach was adapted from our previous synthesis of [^{11}C]4F-MHPG.¹² Purified [^{18}F]4F-MTA was reacted with cyanogen bromide for 3 min at 120°C and subsequently treated with $\text{NH}_4\text{Br}/\text{NH}_4\text{OH}$ for 15 min at 130°C, followed by HPLC purification to afford the final product [^{18}F]4F-MHPG. The structure of the purified product was verified by comparing its retention time against co-injected non-radioactive standard of 4FMHPG using reverse-phase HPLC (Synergy Hydro 4 μ , 250 \times 4.6 mm, 10% EtOH in 60 mM NaH_2PO_4 , 1.1 ml/min, $R_t = 10.4$ min). The total synthesis time from production of [^{18}F]fluoride ion to obtaining the final product was 200–220 min. The overall decay-corrected radiochemical yield was 1–2% with >98% radiochemical purity. The specific activity of [^{18}F]4F-MHPG was 0.3–0.5 Ci/ μmol at the end of synthesis. The radiolabeling steps were not optimized for radiochemical yields and reaction times. Radiochemistry would need to be further improved to optimize production for clinical use of this radiotracer.

Kinetic Studies in Isolated Rat Heart

Uptake rates of [^{18}F]4F-MHPG into sympathetic neurons, as well as the ability of cardiac neurons to retain these compounds, were assessed by performing kinetic studies in an isolated working rat heart preparation, using previously reported methods.¹² In these studies the extraneuronal catecholamine uptake mechanism in the rat heart ('uptake-2') was inhibited by adding 54 μM corticosterone to the heart perfusion buffer.²³ Neuronal uptake rates (K_{up} ; ml/min/g wet) were measured by performing a 10 min infusion of the radiotracer at a constant perfusate concentration into the isolated heart. At the end of the constant infusion period, the heart was switched to normal perfusion buffer for 120 min to measure radiotracer clearance rates (expressed as a clearance half-time, $T_{1/2}$, in h). The kinetics of [^{18}F]4F-MHPG in the isolated rat heart were very similar to those of [^{11}C]4F-MHPG (Figure 2). The neuronal uptake rate of [^{18}F]4F-MHPG in the isolated rat heart was $K_{\text{up}} = 0.68$ ml/min/g wet and neuronal retention times were very long (clearance $T_{1/2} > 13$ h). These values are very similar to those previously observed for [^{11}C]4F-MHPG ($K_{\text{up}} = 0.72$ ml/min/g wet; $T_{1/2} > 73$ h).¹² For comparison, these values, along with K_{up} and $T_{1/2}$ values for [^{123}I]MIBG²⁴, [^{11}C]HED²⁵ and [^{18}F]PFBG²⁶, are shown in Table 1. The slower neuronal uptake rate and very long retention kinetics of [^{18}F]4F-MHPG are consistent with those we targeted as being ideal for tracer kinetic analyses in human PET studies of cardiac sympathetic innervation.¹²

Biodistribution Studies in Rats

The biodistribution of [^{18}F]4F-MHPG into various tissues of the rat at $t = 30$ min after intravenous injection was determined. Biodistribution data for [^{18}F]4F-MHPG were very similar to results previously obtained with [^{11}C]4F-MHPG (Table 2). The ^{18}F -labeled analog exhibited somewhat lower uptake into heart and lung, while distribution of [^{18}F]4F-MHPG into other adrenergically innervated tissues like the spleen and adrenal medulla were very consistent with the results seen with [^{11}C]4F-MHPG. A two-tailed t-test, assuming unequal variances, demonstrated there were no statistically significant differences in the uptake of the two tracers in any organ. For comparison, biodistribution data for [^{125}I]MIBG₁ and [^{11}C]HED¹² are also provided in Table 2. The 4F-MHPG derivatives had lower uptake into left ventricle consistent with their NET transport rates being slower than those of MIBG and HED.

MicroPET Imaging Studies in Rhesus Macaque

The hearts of monkeys²⁷ and humans^{28, 29} lack the extraneuronal uptake (uptake-2) pathway of catecholamines, making the monkey a more appropriate animal model for evaluating sympathetic nerve tracers than the dog, which has significant uptake-2 activity.³⁰ PET imaging with [¹⁸F]4F-MHPG was performed in a rhesus macaque monkey to assess its *in vivo* imaging properties. Cardiac uptake of [¹⁸F]4F-MHPG provided high quality images, with uniform uptake in the left ventricle and final heart-to-blood activity ratios (80–90 min after injection) were 5-to-1. There was essentially no retention of the tracer in the lungs. Uptake of [¹⁸F]4F-MHPG in the liver was a little lower than the cardiac uptake, unlike the relatively high liver uptake seen previously with other sympathetic nerve radiotracers such as MIBG and [¹¹C]HED, resulting in improved overall image quality. There was little or no activity observed in the vertebrae of the spine in sagittal images, suggesting there is little *in vivo* defluorination of the compound. Further work is needed to characterize the kinetics and *in vivo* metabolism of [¹⁸F]4F-MHPG.

In conclusion, [¹⁸F]4F-MHPG was successfully prepared and initial biological studies demonstrated its kinetic properties were consistent with those we targeted as being optimal for tracer kinetic analyses in human PET studies of cardiac sympathetic innervation. MicroPET imaging studies in a monkey provided high quality images of the regional distribution of sympathetic nerves in the heart. These positive initial results demonstrate that [¹⁸F]4F-MHPG is a promising candidate for further development as a radiotracer for clinical PET studies of cardiac sympathetic innervation.

Acknowledgments

We thank the staff of the University of Michigan Cyclotron/PET Facility for their support in the preparation and evaluation of all radiopharmaceuticals included in this work. This work was supported by grant R01-HL079540 from the National Heart Lung and Blood Institute, National Institutes of Health, Bethesda MD USA.

References

1. Wieland DM, Brown LE, Rogers WL, Worthington KC, Wu J-L, Clinthorne NH, Otto CA, Swanson DP, Beierwaltes WH. *J. Nucl. Med.* 1981; 22:22. [PubMed: 7452352]
2. Henneman MM, Bengel FM, van der Wall EE, Knuuti J, Bax JJ. *J. Nucl. Cardiol.* 2008; 15:442. [PubMed: 18513651]
3. Rosenspire KC, Haka MS, Van Dort ME, Jewett DM, Gildersleeve DL, Schwaiger M, Wieland DM. *J. Nucl. Med.* 1990; 31:1328. [PubMed: 2384800]
4. Chakraborty PK, Gildersleeve DL, Jewett DM, Toorongian SA, Kilbourn MR, Schwaiger M, Wieland DM. *Nucl. Med. Biol.* 1993; 20:939. [PubMed: 8298573]
5. Del Rosario RB, Jung Y-W, Chakraborty PK, Sherman PS, Wieland DM. *Nucl. Med. Biol.* 1996; 23:611. [PubMed: 8905825]
6. Wieland DM, Rosenspire KC, Hutchins GD, Van Dort M, Rothley JM, Mislanker SG, Lee HT, CC M, Gildersleeve DL, Sherman PS, Schwaiger M. *J. Med. Chem.* 1990; 33:956. [PubMed: 2308146]
7. Ding Y-S, Fowler JS, Dewey SL, Logan J, Schlyer DJ, Gatley SJ, Volkow ND, King PT, Wolf AP. *J. Nucl. Med.* 1993; 34:619. [PubMed: 8455079]
8. Loc'h C, Mardon K, Valette H, Brutesco C, Merlet P, Syrota A, Mazière B. *Nucl. Med. Biol.* 1994; 21:49. [PubMed: 9234263]
9. Garg PK, Garg S, Zalutsky MR. *Nucl. Med. Biol.* 1994; 21:97. [PubMed: 9234270]
10. Raffel DM, Wieland DM. *Nucl. Med. Biol.* 2001; 28:541. [PubMed: 11516699]
11. Green AL, Fielden R, Bartlett DC, Cozens MJ, Eden RJ, Hills DW. *J. Med. Chem.* 1967; 10:1006. [PubMed: 6056024]
12. Raffel DM, Jung YW, Gildersleeve DL, Sherman PS, Moskwa JJ, Tluczek LJ, Chen W. *J. Med. Chem.* 2007; 50:2078. [PubMed: 17419605]

13. Su W. *Synth. Comm.* 1996; 26:407.
14. Ma D, Wu W, Yang G, Li J, Li J, Ye Q. *Bioorg. Med. Chem. Lett.* 2004; 14:47. [PubMed: 14684295]
15. Langer O, Dollé F, Valette H, Halldin C, Vaufrey F, Fuseau C, Coulon C, Ottaviani M, Någren K, Bottlaender M, Mazière B, Crouzel C. *Bioorg. Med. Chem.* 2001; 9:677. [PubMed: 11310603]
16. Schoeps KO, Halldin C, Någren K, Swahn CG, Karlsson P, Hall H, Farde L. *Nucl. Med. Biol.* 1993; 20:669. [PubMed: 8358354]
17. Ding Y-S, Fowler J, Gatley S, Dewey S, Wolf A. J. *Med. Chem.* 1991; 34:767. [PubMed: 1995899]
18. Inbasekaran MN, Mangner TJ, Wieland DM. *J. Labeled Compds. Radiopharm.* 1983; 20:1201.
19. Poss MA, Iwanowicz E, Reid JA, Lin J, Gu Z. *Tetrahedron Lett.* 1992; 33:5933.
20. Iwanowicz E, Poss MA, Lin J. *Synthetic Comm.* 1993; 23:1443.
21. Bernatowicz MS, Wu Y, Matsueda GR. *J. Org. Chem.* 1992; 57:2497.
22. Vaidyanathan G, Affleck DJ, Zalutsky MR. *J. Med. Chem.* 1994; 37:3655. [PubMed: 7932592]
23. Salt PJ. *Eur. J. Pharmacol.* 1972; 20:329. [PubMed: 4643454]
24. DeGrado TR, Zalutsky MR, Coleman RE, Vaidyanathan G. *Nucl. Med. Biol.* 1998; 25:59. [PubMed: 9466363]
25. DeGrado TR, Hutchins GD, Toorongian SA, Wieland DM, Schwaiger M. *J. Nucl. Med.* 1993; 34:1287. [PubMed: 8326386]
26. Berry CR, Garg PK, Zalutsky MR, Coleman RE, DeGrado TR. *J. Nucl. Med.* 1996; 37:2011. [PubMed: 8970525]
27. Carr EA, Carroll M, Counsell RE, Tyson JW. *Br. J. clin. Pharmacol.* 1979; 8:425. [PubMed: 116669]
28. Dae MW, De Marco T, Botvinick EH, O'Connell W, Hattner RS, Huberty JP, Yuen-Green MS. *J. Nucl. Med.* 1992; 33:1444. [PubMed: 1634934]
29. Glowniak J, Turner F, Gray L, Palac R, Lagunas-Solar M, Woodward W. *J. Nucl. Med.* 1989; 30:1182. [PubMed: 2661758]
30. Eisenhofer G, Smolich JJ, Esler MD. *Naunyn-Schmiedeberg's Arch. Pharmacol.* 1992; 345:160. [PubMed: 1570020]

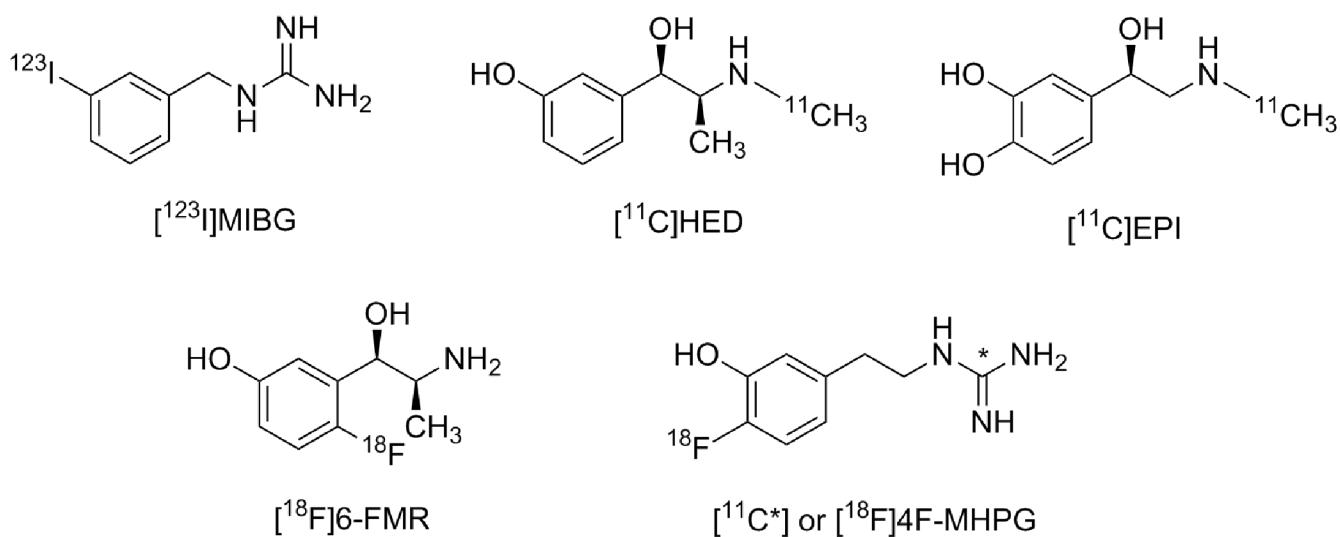


Figure 1.
Structures of cardiac sympathetic nerve imaging agents.

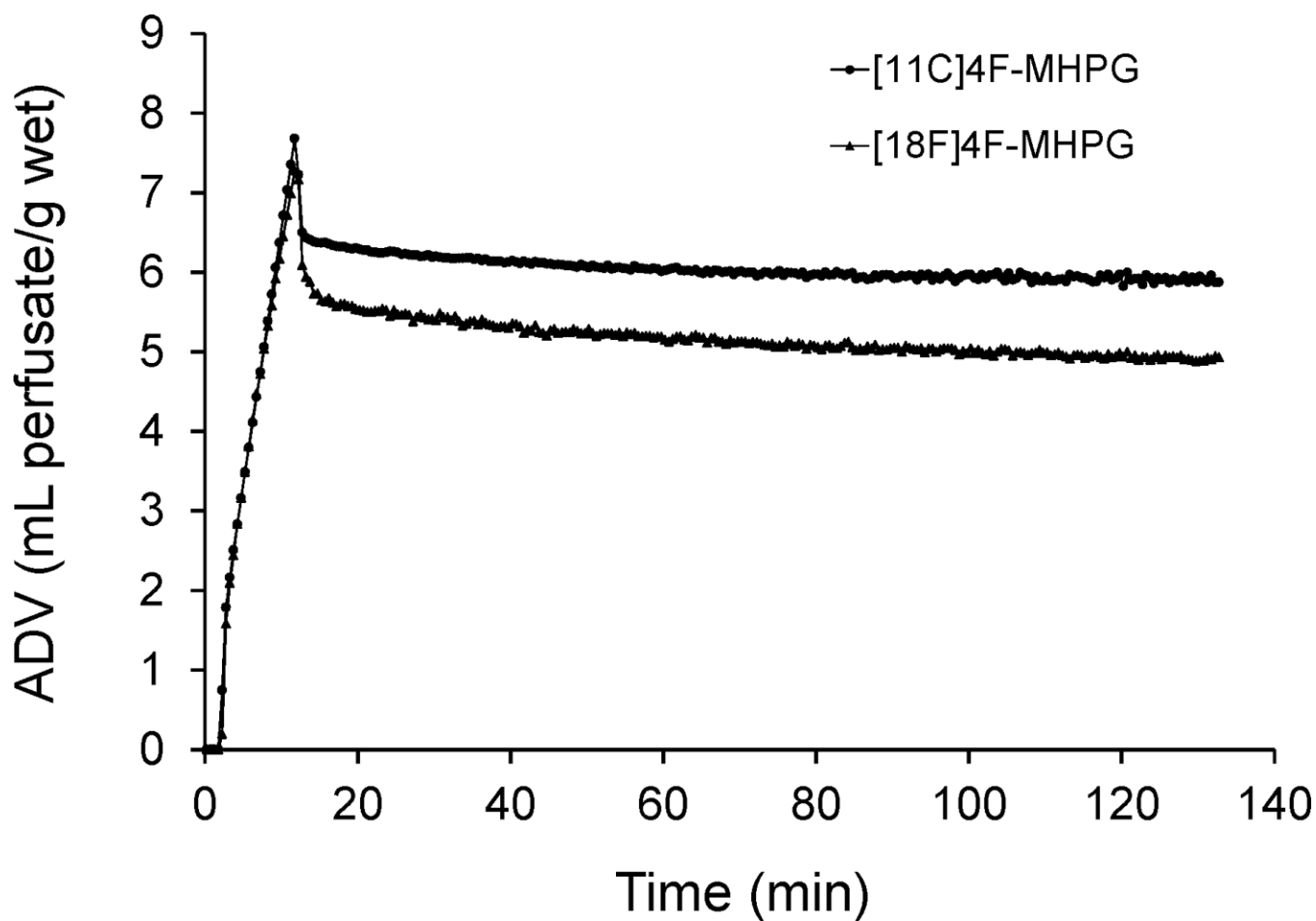
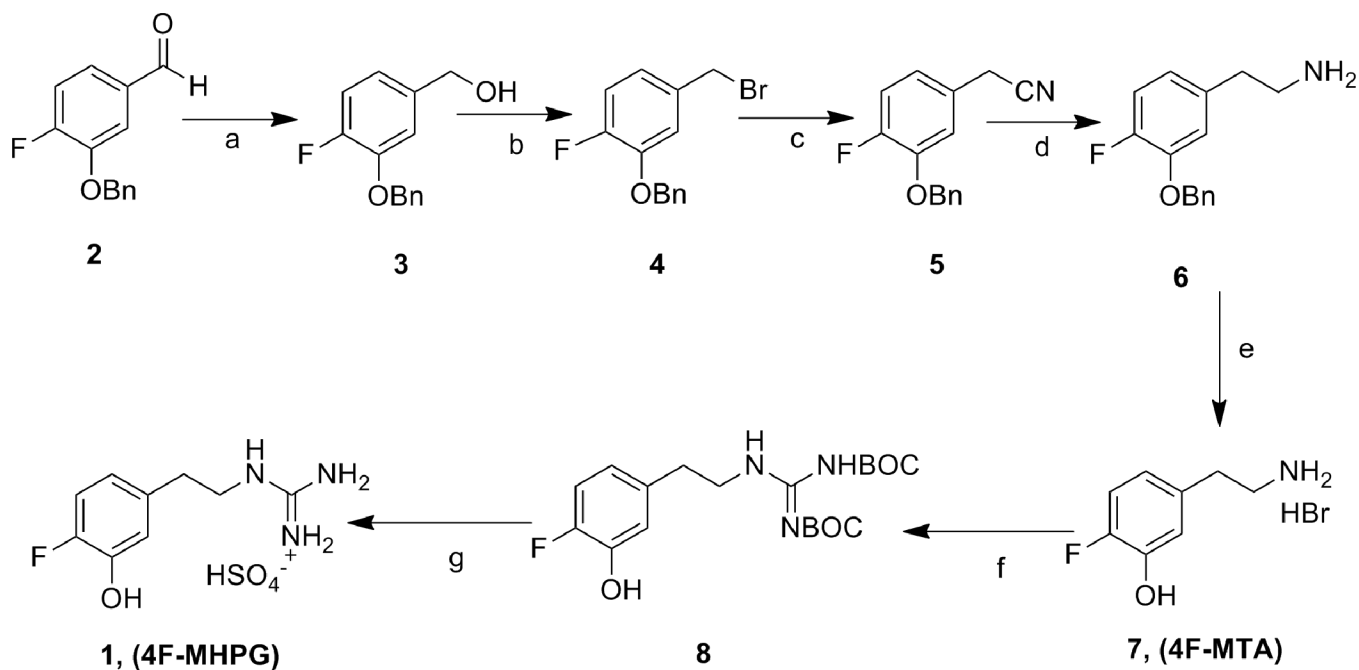
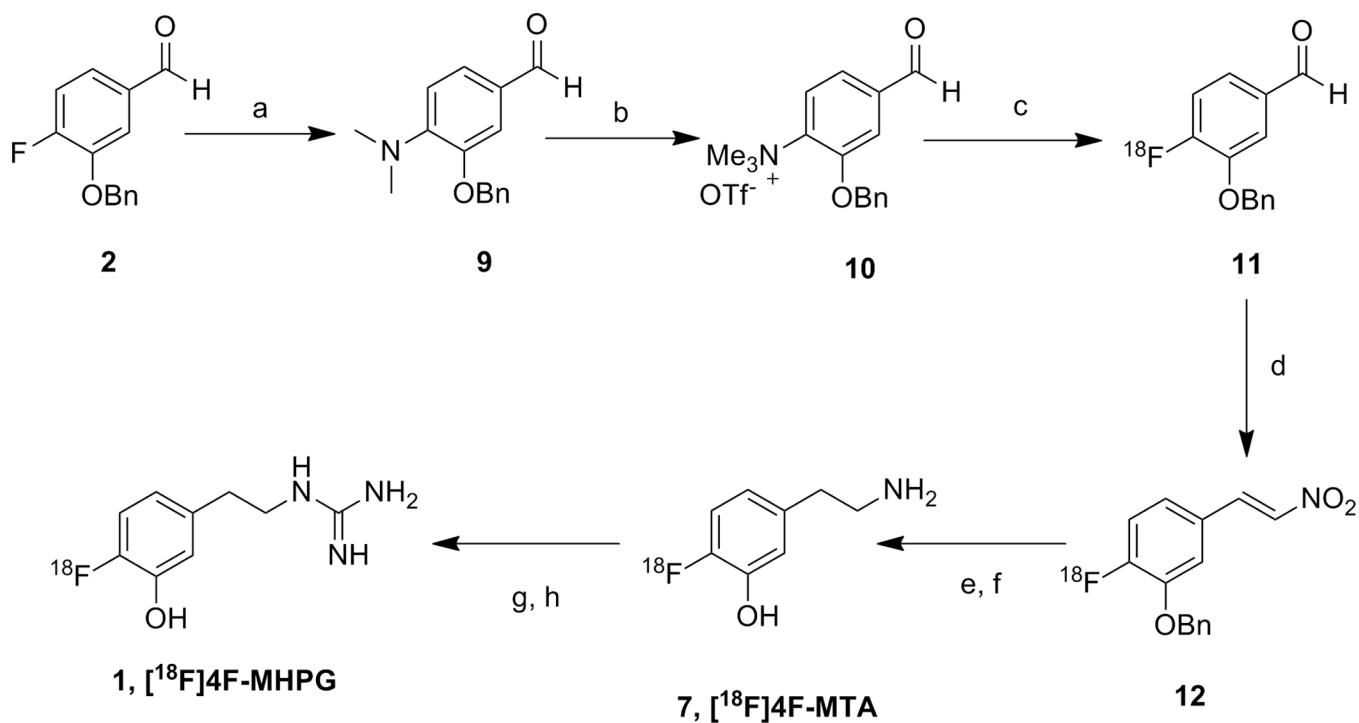


Figure 2. Kinetics of [^{11}C]4F-MHPG and [^{18}F]4F-MHPG in the isolated rat heart. A 10-min constant infusion study assesses the neuronal uptake rate of the tracer into sympathetic nerve terminals, after which the heart is switched back to normal heart perfusate to study clearance rates. Both tracers exhibit very long neuronal retention times due to sequestration inside norepinephrine storage vesicles.

**Scheme 1.**

a) NaBH₄, THF, 0°C-rt, N₂, 4 h, 72%; b) PBr₃, CH₂Cl₂, rt, overnight, 37%; c) NaCN, DMSO, rt, 3 h, 90%; d) 1.0 M BH₃-THF complex, THF, reflux, 2 h, 69%; e) HBr (48%), 130°C, N₂, 6 h, 97%; f) 1,3-bis(*tert*-butoxycarbonyl)-2-methyl-2-thiopseudourea, HgCl₂, Et₃N, DMF, 0°C-rt, 24 h, 87%, g) 1.0 N HCl, CH₂Cl₂/MeOH, rt, 24 h, 87%.

**Scheme 2.**

a) Dimethylamine hydrochloride, K₂CO₃, DMSO:H₂O (2.5:1), 110°C, overnight, 82%; b) CH₃OTf, CH₂Cl₂, N₂, rt, overnight, 71%; c) [¹⁸F]F⁻-Kryptofix-2.2.2; d) CH₃NOS, NH₄OAc, MeOH/AcOH; e) BH₃/LAH; f) 48% HBr; g) CNBr (5.0M in CH₃CN); h) NH₄Br/NH₄OH.

Table 1Neuronal uptake rates (K_{up}) and major clearance half-times ($T_{1/2}$) in isolated rat hearts*.

Tracer	Acronym	K_{up} (ml/min/g wet)	Major Clearance $T_{1/2}$ (h)	Ref.
[¹²³ I]- <i>m</i> -iodobenzylguanidine	[¹²³ I]MIBG	3.6 ± 0.2	3.5 ± 1.8	[24]
[¹¹ C]-(-)- <i>m</i> -hydroxyephedrine	[¹¹ C]HED	2.7 ± 0.4	1.1 ± 0.3	[25]
<i>p</i> -[¹⁸ F]fluorobenzylguanidine	[¹⁸ F]PFBG	1.2 ± 0.4	0.53 ± 0.06	[26]
[¹¹ C]4-fluoro- <i>m</i> -hydroxyphenethylguanidine	[¹¹ C]4F-MHPG	0.72	> 73	[12]
[¹⁸ F]4-fluoro- <i>m</i> -hydroxyphenethylguanidine	[¹⁸ F]4F-MHPG	0.68	> 13	This work

* Extraneuronal uptake (uptake-2) was blocked pharmacologically.

Table 2

Tissue concentrations at $t = 30$ min in rats (% injected dose/g, $n = 5$ each).

Tracer	left ventricle	lung	liver	spleen	adrenal medulla	blood	Ref.
[¹²⁵ I]MIBG	3.63 ± 0.20	2.31 ± 0.19	1.19 ± 0.06	0.85 ± 0.06	1.53 ± 0.08	0.10 ± 0.01	[11]
[¹¹ C]HED	2.85 ± 0.42	0.40 ± 0.12	2.32 ± 0.25	1.31 ± 0.14	0.72 ± 0.08	0.08 ± 0.01	[12]
[¹¹ C]4F-MHPG	1.77 ± 0.27	0.56 ± 0.15	1.22 ± 0.18	0.52 ± 0.10	0.56 ± 0.21	0.08 ± 0.01	[12]
[¹⁸ F]4F-MHPG	1.45 ± 0.13	0.43 ± 0.08	1.14 ± 0.16	0.56 ± 0.10	0.54 ± 0.08	0.07 ± 0.01	This work

Values are mean ± SD.